PERSISTENT AND RESURGENT VOLTAGE-GATED SODIUM CURRENTS IN MOUSE VESTIBULAR GANGLION NEURONS

Selina Baeza Loya, Ruth Anne Eatock

Department of Neurobiology, University of Chicago, Chicago IL

MOTIVATION: Vestibular ganglion neurons (VGN) are the cell bodies of primary vestibular afferents in the inner ear. Expression of different ion channels affects VGN **firing properties** that contribute to encoding of sensory stimuli. The impact of diverse voltage-gated sodium (**Na_V**) **currents** on action potential waveforms and firing patterns remains unknown.

APPROACH: Tetrodotoxin (TTX)-sensitive Na_V currents were recorded from isolated, cultured mouse VGN with the whole cell patch clamp technique. **Voltage step protocols** revealed voltage and time dependence. **Action potential clamp** revealed Na_V flow during the spike waveform. **Current clamp** investigated firing patterns and spike trains.

RESULTS AND CONCLUSIONS: Persistent Na_V and **resurgent Na_V currents** were observed during postnatal development, as firing patterns mature, and are likely carried through **$Na_V1.6$**. Such currents may regulate sustained (regular) firing patterns. They add complexity to VGN Na_V currents, already known to involve TTX-Sensitive, TTX-Insensitive, and TTX-Resistant Na_V α-subunits.

1. *VGN encode head motions with different firing patterns*

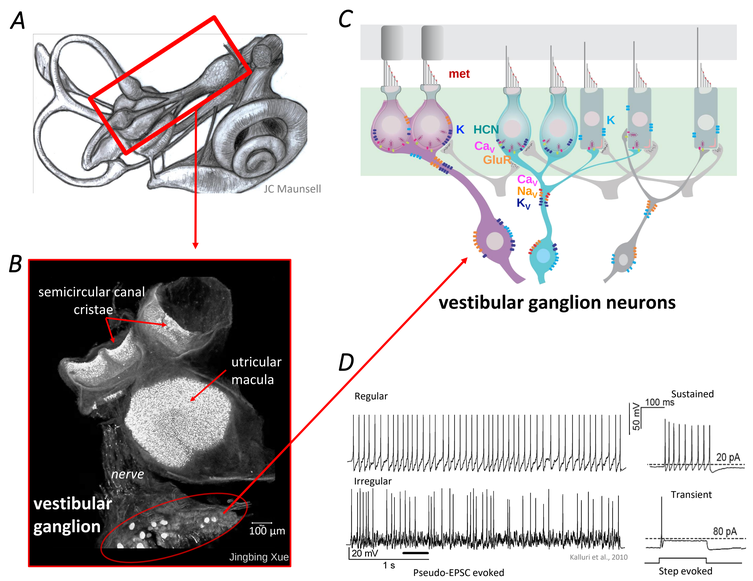

A-C) VGN innervate hair cells of vestibular epithelia and convey information about head position and head motions to the brain.

D) VGN innervating peripheral and central epithelial zones have **regular** and **irregular timing of action potentials (APs)**, corresponding to rate and temporal encoding strategies, respectively (Jamali et al., 2016), suited to different kinds of head motion. Regular and irregular afferents generate **sustained** and **transient** firing patterns in response to current steps. Differences in expression of K channels contribute to these differences in AP timing (Kalluri et al., 2010).

2. *How do diverse Na_V currents in VGN shape firing?*

Rat VGN express multiple multiple voltage-gated sodium (Na_V) pore-forming (α) subunits that pass ***transient Na_V current (Na_VT)*** (Liu et al., 2016), including TTX-Insensitive ($Na_V1.5$) and TTX-Resistant ($Na_V1.8$) currents, plus two TTX-Sensitive currents. TTX-S channels include $Na_V1.6$ channels (Meredith & Rennie 2018) which are expressed at afferent hemi-nodes below the hair cells (Lysakowski et al., 2011).

Na_V currents can also take ***persistent*** and ***resurgent*** forms (***Na_VP, Na_VR***) which can be significant near AP threshold, affecting neuronal excitability (Raman & Bean 1997). We hypothesize that differences in expression of ***Na_VP*** and ***Na_VR*** contribute to differences in regularity of firing between VGN.

3. *Whole-cell patch clamp recording of Na_V currents from VGN*

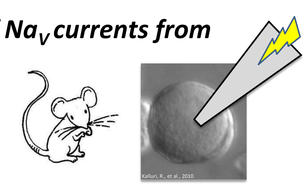

VGN from CD1 mice (P3-P25, average age P13) are enzymatically and mechanically dissociated, then cultured overnight.

Whole cell ruptured-patch clamp

Voltage clamp protocols: *steps, ramps, APs;* Cs^+ internal and external solutions (reduced Na^+; Ca^{2+} free; K^+ blockers), unless otherwise specified; Na_V current isolated by subtraction of records in 1 µM TTX from records in 0 TTX.

Current clamp protocols: *Steps; trains of synthetic EPSCs with pseudo-random timing to examine spike timing regularity* (Kalluri et al., 2010); standard internal (high K+, Cl-) and external solutions (high Na+, Cl-)

Local perfusion of **4,9-anhydro-tetrodotoxin** (4,9-ah-TTX) ($Na_V1.6$ channel blocker)

4. *VGN have Transient (Na_VT), Persistent (Na_VP) and Resurgent (Na_VR) currents*

A) I-Na_VT

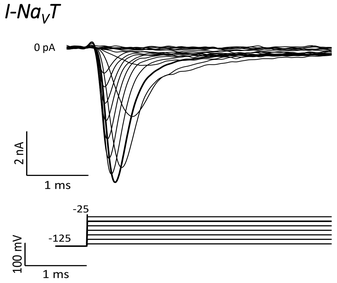

B) I-Na_VP

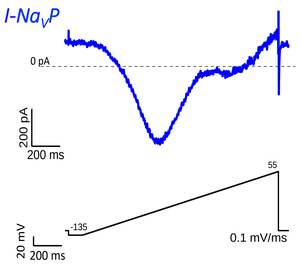

C) I-Na_VR

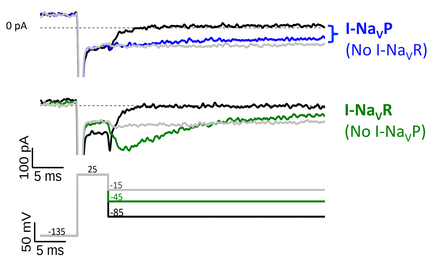

D) I-Na_VT, I-Na_VR, I-Na_VP I-V relations

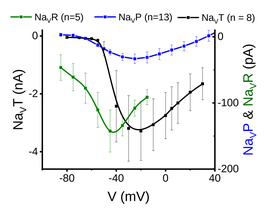

E) I-Na_VR, I-Na_VP vs. Age

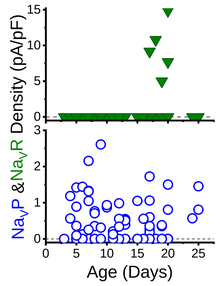

Cs^+ solutions; Na_V current isolated by 1-µM TTX subtraction.
A) Na_VT voltage step protocol. All cells had I-Na_VT.
B) Na_VP voltage ramp protocol. Of 100 cells tested (P3-25) (see ***E***), 62 had I-Na_VP.
C) Na_VR voltage step protocol. VGN with I-Na_VP: P20; VGN with I-Na_VR: P18. Of 81, 5 (all >P17, see ***E***) showed I-Na_VR.
D & E) Voltage dependence and development of I-Na_VP and I-Na_VR similar to reports from spiral ganglion (Browne et al., 2017).

5. *Na_VT and Na_VP currents blocked by $Na_V1.6$-specific blocker, 4,9-ah-TTX*

A) Partial block of I-Na_VT

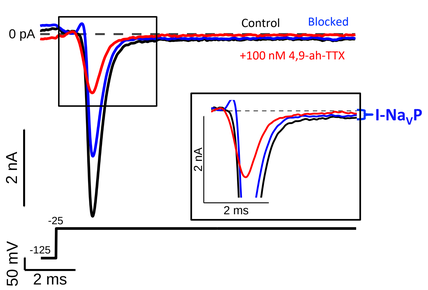

B) Activation and Inactivation Curves

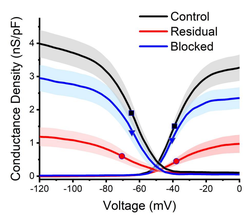

72.3 ± 5.6% block of I-Na_VT Gmax density ; 100% block I-Na_VP in Cs^+ solutions using voltage ramp protocol (n=13)

C) Full block of I-Na_VP

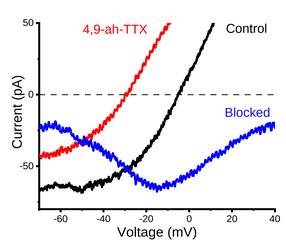

$V_{1/2}$	Act Mean ± SE (mV) (n=12)	Inact Mean ± SE (mV) (n=11)
Control ■	-38.7 ± 1.2	-68.1 ± 2.4
Unblocked ●	-42.3 ± 2.2	-78.4 ± 3.3*
Blocked ◀	-39.4 ± 1.4	-68.4 ± 2.1

Table 1: Voltage Dependence of Activation and Inactivation. *Unblocked I-Na_VT current has more negative voltage dependence for inactivation (*P=0.03; Cohen's d = 0.98*).

6. *Blocking $Na_V1.6$ current alters VGN spiking*

A) Action potentials

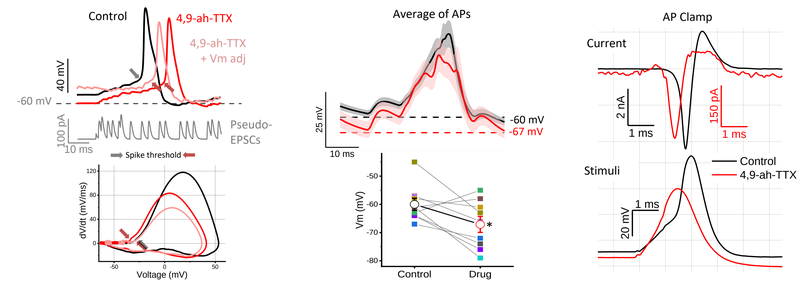

Left: AP evoked by synthetic ("pseudo-") EPSCs has more negative voltage threshold In 4,9-ah-TTX (red) than in control (black). Phase Plane Plot, bottom. Adjusting resting membrane potential (Vm) to pre-drug levels (thin pink line) restored voltage threshold. ***Middle:*** Average of AP waveforms (n=9) aligned on pseudo-EPSCs; Vm usually hyperpolarized in Nav1.6 blocker. ***Right:*** AP clamp, physiological solutions: APs collected in 4,9-ah-TTX evoked smaller, more negatively-activating currents relative to AP recorded without the drug (black).

B) Step-evoked firing pattern

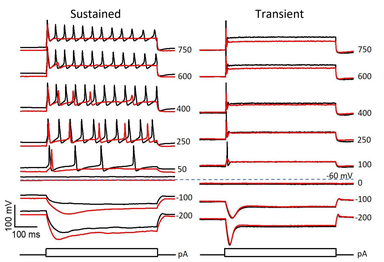

	Vm (mV) ± SE	Step threshold (pA)	Spike Height (mV)	Spike Width (ms)	Threshold @ dV/dt = 5 (mV)	Peak dV/dt
CONTROL (n = 9)	-60.0 ± 2.1	100.0 ±17.6	61.7 ± 6.9	3.2 ± 0.6	-42.8±2.1	55.0 ±19.1
DRUG (n = 9)	-67.1 ± 2.8	183.3 ± 28.8	50.4 ± 7.2	4.5 ± 0.7	-50.4±4.0	39.7±17.0
P-value	0.04*	0.03*	0.07	0.07	0.09	0.33

Table 2: **Parameters of firing patterns and APs**. *After 4,9-ah-TTX, V_m hyperpolarized (*Cohen's d = 0.95*), and step current injection threshold increased (*1.7*).

In 100 nM 4,9-ah-TTX (red traces), excitability decreases relative to control (black) during step current injections.

C) AP trains evoked by pseudo-EPSCs

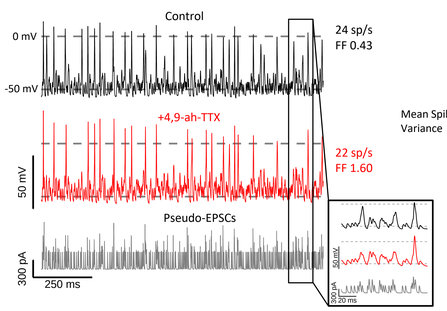

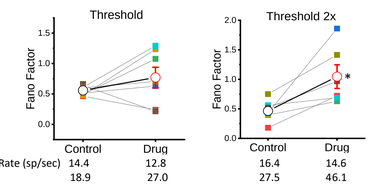

	Control	Drug
Mean Spike Rate (sp/sec)	14.4	12.8
Variance	18.9	27.0
	16.4	14.6
	27.5	46.1

AP regularity was altered by 4,9-ah-TTX; same pseudo-EPSCs (*left*) evoked AP trains. Events peaking >0 mV counted as spikes. Pseudo-EPSCs based on cochlear waveforms; from R. Kalluri.

*Fano factor (a measure of irregularity, $FF = \frac{\sigma^2}{\mu}$) increases with suprathreshold stimulation in 4,9-ah-TTX as variance increases (*right*) (n=7) (*P=0.03*).

7. *Summary*

Na_V currents in mouse VGN have multiple modes: transient, persistent, and resurgent. As in cochlear ganglion neurons (Browne et al., 2017), resurgent currents were not detected in the first postnatal week. Persistent and resurgent currents may be carried by $Na_V1.6$ channels (Raman et al., 1997). In VGN, persistent and resurgent currents may influence firing patterns of maturing afferents: blocking transient and persistent $Na_V1.6$ currents may change AP waveform, AP current and voltage thresholds, mean firing rate, and regularity of firing.

References

Browne L, Smith KE, Jagger DJ (2017) Identification of persistent and resurgent sodium currents in spiral ganglion neurons cultured from the mouse cochlea. Nov 14;4(6).

Gittis AH, du Lac S (2008) Similar Properties of Transient, Persistent, and Resurgent Na Currents in GABAergic and non-GABAergic Vestibular Nucleus Neurons. J Neurophysiol 99: 2060-2065

Jamali M, Chacron MJ, Cullen KE (2016) Self-motion evokes precise spike timing in the primate vestibular system. *Nat Comm* 7:13229.

Kalluri R, Xue J, Eatock RA (2010) Ion channels set spike timing regularity of mammalian vestibular afferent neurons. *J Neurophysiol* 104: 2034–51.

Liu XP, Wooltorton JRA, Gaboyard-Niay S, Yang FC, Lysakowski A, Eatock RA (2016) Sodium channel diversity in the vestibular ganglion: Nav1.5, Nav1.8, and tetrodotoxin-sensitive currents. *J Neurophysiol* 115: 2536–55.

Lysakowski A, Gaboyard-Niay S, Calin-Jageman I, Chatlani S, Price SD, Eatock RA (2011) Molecular microdomains in a sensory terminal, the vestibular calyx ending. *J Neurosci* 31(27):10101-10114

Meredith FL, Rennie KJ (2018) Regional and developmental differences in Na+ Currents in vestibular primary afferent neurons. *Frontiers* 12:423

Raman IM, Bean BP (1997) Resurgent sodium current and action potential formation in dissociated cerebellar purkinje neurons. *J Neurosci* 17:4517–26.

Raman IM, Sprunger L, Meisler MH, Bean BP (1997) Altered subthreshold sodium current and disrupted firing patterns in Purkinje Neurons of *Scn8a* mutant mice. *Neuron* 19:881-891.

Acknowledgments: Thanks to R. Kalluri for pseudo-random EPSC stimulation protocol.

Funded by NIDCD, HHMI Gilliam